ACS OMEGA

Open Access

http://pubs.acs.org/journal/acsodf

Article

Enhancement of the Electroluminescence and Strain Properties of Dielectric Elastomeric Actuators Using Liquid Metal Reflectors

Jongyeop An,[§] Beomgil Ha,[§] Seon Namgung, and Byung Yang Lee*

Cite This: *ACS Omega* 2024, 9, 3916−3922

Read Online

ACCESS | Metrics & More | Article Recommendations | Supporting Information

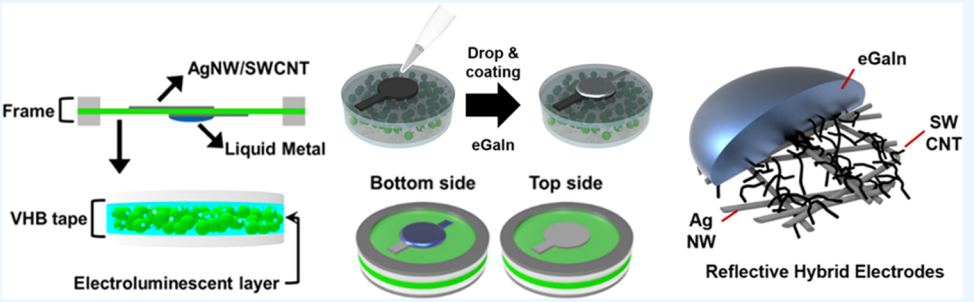

ABSTRACT: We report on the enhancement of the light-emitting and mechanical performance of multifunctional dielectric elastomeric actuators by combining liquid eutectic gallium indium metal with a stretchable and transparent hybrid electrode composed of silver nanowires (AgNWs) and carbon nanotubes (CNTs). The device shows improved optical properties, electrical conductivity, and stability for electroluminescent dielectric elastomer actuators compared with previous works. Combining single-walled CNTs (SWCNTs) with AgNWs impeded the chemical reaction between the liquid metal and AgNWs, resulting in a more stable operation of the device. The maximum luminance and maximum strain of the electroluminescent dielectric elastomer actuator increased by 50% (from 300 to 450 cd m^{-2}) and 44% (from 85 to 122%), respectively.

1. INTRODUCTION

Devices based on soft materials are gaining increased interest owing to their expected applications in soft robotics and wearable electronics, such as artificial muscles or flexible luminescent devices.[1−5] Among these, multifunctional devices based on soft materials are being developed to realize a combination of the above functionalities in a single device, exemplified by soft actuating speakers and lens actuators.[6−9] In particular, we recently reported an electroluminescent dielectric elastomeric actuator (ELDEA) with multiple functionalities that exhibits both actuation and light-emitting capabilities.[10] Our results showed that when the alternating current (AC) and direct current (DC) signal amplitudes were increased, both the luminance and strain values could be increased. However, at increased AC and DC signal amplitudes, we observed a decrease in the luminance at large strains and a device failure at high frequencies. Therefore, improving the strain behavior and simultaneously lowering the required driving voltage for ELDEA operation is necessary. Herein, we propose an effective strategy for improving the mechanical and optical performance of ELDEAs based on the use of a hybrid composite electrode that combines liquid metal (eutectic gallium indium, eGaIn) with a stretchable and transparent silver nanowire (AgNW)/carbon nanotube (CNT) hybrid electrode. In particular, stretchable electrodes composed of AgNW/CNTs composite are reported to have high performance.[11,12] Given that eGaIn has benign properties such as negligible vapor pressure at room temperature 25 °C (~10^{-4} at 540 °C),[13] its suitable properties for stretchable electrodes (low-melting point of 15.7 °C),[14] high electrical conductivity (3.4 × 10^4 S·cm^{-1}),[15] and high self-healing ability,[16] our AgNW/CNT/liquid metal (ACLM) electrodes are optimal in improving the performance of the ELDEAs. This ACLM electrode enhances both the electroluminance efficiency and stretchability performance of the ELDEA. Additionally, the use of eGaIn in our ACLM electrodes resulted in an effective decrease in the required AC and DC signal levels for a given strain and electroluminescence level. As a result, it was confirmed that the maximum luminance and maximum strain characteristics of the electroluminescent dielectric elastomer actuator were increased by 50% (from 300 to 450 cd m^{-2}) and 44% (from 85 to 122%), respectively, compared to previous studies. This was possible by using eGaIn as a light reflector to improve the characteristics of ELDEA. It should be noted that this is the first report on the

Received: October 20, 2023
Revised: December 18, 2023
Accepted: December 25, 2023
Published: January 11, 2024

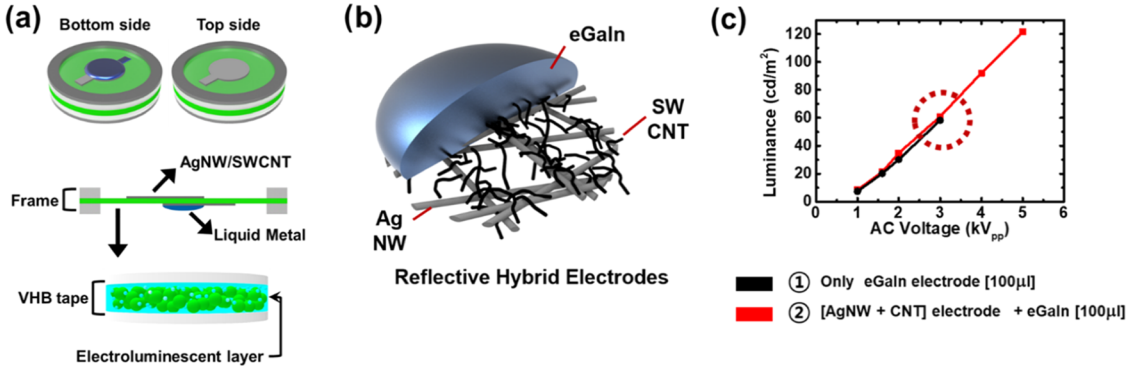

Figure 1. Schematic of the fabrication of the electroluminescent dielectric elastomer actuator (ELDEA) device and the AgNW/CNT/liquid metal (ACML) electrodes. (a) ELDEA structure. (b) Schematic of the ACML hybrid electrode. The CNTs protect the AgNWs from reacting with eGaIn. (c) Breakdown voltage depending on the electrode structure.

application of eGaIn specifically for enhancing ELDEA luminescence and stretchability. Our findings can contribute to providing new strategies for guiding optical signals and enhancing the electroluminescence of light-emitting actuators.

2. EXPERIMENTAL SECTION

2.1. Fabrication of AgNW/SWCNT/eGaIn Hybrid Electrode. The fabrication of the AgNW/SWCNT electrode was based on a prior study.[17] Briefly, a 1 wt % AgNW (length 22 μm, diameter 23 nm) suspension in deionized water was diluted to a target concentration (2 mg mL^{-1}) with DI to a 50 mL solution. SWCNTs (0.2 ng mL^{-1}) were diluted into sodium dodecyl sulfate (SDS, 50 mL, 5 wt %) with DI water. The prepared AgNWs and SWCNT solutions (50 mL) were vacuum-filtered through a polycarbonate filter (pore size of 0.08 μm, radius of 47 mm, Whatman). After vacuum filtration, the AgNW/SWCNT hybrid electrodes were dried in air. For the reflective electrode, eGaIn (100 μL, ≥99.99% trace-metal basis, Sigma-Aldrich) was dropped on the AgNW/SWCNT hybrid electrodes.

2.2. Fabrication of DEA and ELDEA. For DEA fabrication, a dielectric elastomer (VHB Tape 4910) was pre-stretched radially three times so that its area increased 9 times compared to the original area and was fixed to a circular acrylic frame (diameter, 60 mm). Then, we transferred the premanufactured AgNW/CNT hybrid electrodes on both sides of the elastomeric device. Next, we attached the released paper mask of the electrode on the device and then dropped the liquid metal (100 μL, eGaIn, ≥99.99% trace-metal basis, Sigma-Aldrich) on the mask. We then pasted the drop of liquid metal along the mask. Finally, we removed the mask.

For the fabrication of the ELDEA, a dielectric elastomer (0.5t VHB Tape 4905, 3M) was pre-stretched as in DEA fabrication. Silicon elastomer (Ecoflex 00-50, Smooth-On) was mixed with ZnS/Cu EL particles (size of 9 μm, Shanghai KPT Company) and $BaTiO_3$ NPs for EL amplification. Next, the composite Ecoflex/EL particle mix was spin-coated on the pre-stretched VHB tape at 5500 rpm for 15 s. Finally, another pre-stretched VHB tape was overlaid on the spin-coated VHB tape structure. On one side, an AgNW/SWCNT electrode was transferred. On the other side, an AgNW/SWCNT/eGaIn hybrid electrode was formed.

2.3. Contact Resistance between eGaIn and AgNW/SWCNT Electrode with Two- and Four-Point Probe Experiment. Two- and four-point probe measurements were performed to measure the composite AgNW/SWCNT resistance and the AgNW/SWCNT and eGaIn contact resistance (Figure S1). We used a sourcemeter (2636A, Keithley, USA) for current sourcing and a digital multimeter (34401A, Agilent Technologies) for voltage readouts. The two-point probe measurement gave us information on the sample resistance including the contact resistance between the probe and the sample ($R_{tot} = R_c + R_{ele}$) while the four-point probe measurement gave us information on the tested sample ($R_{tot} = R_{ele}$). Here, R_c is the contact resistance and R_{ele} is the AgNWs + SWCNT resistance.

2.4. ELDEA Actuation and Luminance Measurements. The electroluminescence experiments were performed by applying a combined AC and DC signal to the sample. A combined AC + DC electrical signal was synthesized by using a Tektronix AFG1022 function generator. This signal was applied to a Trek 10/10B-FG high-voltage amplifier (gain G = 606). The output of the high-voltage amplifier was a combined AC and DC signal with DC and AC ranges of 0−8 kV and 1−5 kV_{pp}, respectively. The luminance values were measured using a TES-137 luminance meter, and changes in the electrode area were observed using a USB camera (SC-FD110B, Samsung, Korea).

3. RESULTS AND DISCUSSION

Figure 1a shows the device fabrication schematic. Our ELDEA was fabricated by sandwiching an electroluminescent structure between two electrodes. For the electroluminescent structure, a very high bond (VHB) tape was stretched radially three times and was attached to an acryl frame (outer diameter 60 mm). An electroluminescent layer composed of ZnS/Cu electroluminescent particles embedded in the polymer matrix of Ecoflex was spin-coated on the VHB tape. Then, another pre-stretched VHB tape was laid on the EL layer to make a sandwich structure. Finally, two stretchable and conductive electrodes were formed on each face of the sandwiched structure. These two electrodes differed in their compositions and properties. The electrode on the electroluminescent face was a transparent stretchable electrode composed of a hybrid structure of AgNWs and SWCNTs fabricated using methods reported before, whereby a network of AgNWs is reinforced mechanically and electrically by the SWCNTs.[10] The other electrode, the reflective face, is the ACLM electrode, where the aforementioned AgNW/SWCNT network is coated with eGaIn. The eGaIn improves the physical and optical performance of the electrode. For the optically luminescent face, a transparent AgNW/SWCNT hybrid electrode was

https://doi.org/10.1021/acsomega.3c08246
ACS Omega 2024, 9, 3916−3922

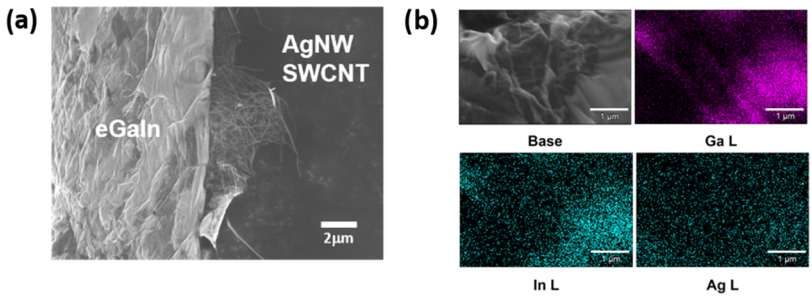

Figure 2. Structure of AgNW/CNT/liquid metal (ACLM) hybrid electrodes. (a) Scanning electron microscopy image of the cross section of an ACLM electrode. The AgNW/SWCNT structure is exposed on the edge of the cross section. (b) Energy-dispersive X-ray (EDX) image of ACLM electrodes.

transferred on the pre-stretched VHB tapes. In the case of the reflective face, we performed the same procedure as the first electrode, and then we spread 100 μL of eGaIn layer to serve as both a reflector and a stretchable electrode. When a combined signal of AC and DC was applied to ELDEA, the device showed both luminescent and stretchable behaviors.

Before AC+DC signals were applied to the electrodes, the chemical stability of the ACLM electrode was studied. Several publications have reported that eGaIn can damage the AgNWs by dissolving the Ag materials.[18] Previous research showed that graphene, which is an sp^2-bond-based carbon material, can prevent Ag dissolution.[19,20] In addition, a spray-coated multilayer of SWCNTs on AgNWs or nanoparticles (NPs) has been reported to provide an adequate physical and chemical barrier, protecting AgNWs and NPs from the reaction with eGaIn.[21−23] Figure 1c shows the effect of using ACLM electrodes on luminance performance. Both had AgNW/SWCNT electrodes as the top electrode. Here, the bottom electrode was either just eGaIn (no AgNW/CNTs) or the ACLM electrode. For the case of the bottom electrode made of only eGaIn (Figure 1c, black), the maximum applicable AC signal amplitude and its corresponding luminance were reduced by over 50% compared to the values measured with the ACLM bottom electrode (Figure 1c, red). The relatively lower level of the maximum applicable AC amplitude can be explained by the penetration of eGaIn into the polymer matrix, which results in electric breakdown of the device occurring at lower voltages, as indicated by the red dotted circle in Figure 1c. The SWCNTs encapsulating the AgNWs protected the AgNWs from a chemical reaction with eGaIn in which Ga dissolved Ag and made the AgNW/SWCNT/eGaIn hybrid electrode a stable, highly stretchable, and reflective surface for ELDEAs (Figures 1b and 2a). The scanning electron microscopy (SEM) image in Figure 2a confirms that the SWCNT layer using the vacuum filtration coating was much thinner than the previously reported spray coating method. Also, in Figure 2, it can be further confirmed from the image that the AgNWs were not dissolved by eGaIn.

The mechanical deformation of ELDEA under a DC signal is due to Maxwell stress between the two electrodes under a static electric field.[24] The electric field in the dielectric is about 23 V μm^{-1} based on the total thickness of the VBH layer and the EL layer of 216 μm and the applied voltage of 5 kV. This electric field value is comparable to that of other reports where the electric field in the dielectric material was calculated to be in the range of 3−10 V μm^{-1}.[9,25−27] To achieve a uniform electric field distribution, intimate electrical contact between the AgNW/CNT film and eGaIn is important. To observe the electrical contact between eGaIn and the AgNW/SWCNT film, we measured the contact resistance between the eGaIn and the AgNW/SWCNT by using two- and four-point probe resistance measurements (Figure S1).[28] Here, a linear channel pattern (22 mm length, 3 mm width) of the AgNW/CNT composite was formed on a solid SiO_2 insulating surface. Afterward, the AgNW/CNT channel was electrically contacted with four eGaIn electrodes with 3 mm spacings. The obtained two-point probe resistance was 32.4 Ω, and the four-point resistance was 32.2 Ω. Using the relation between the two probe resistance ($R + 2R_c$) and the four-probe resistance, the contact resistance (R_c) between AgNW/CNT and eGaIn was extracted to be approximately 0.1 Ω. This value is lower than other reported values of 0.253 Ω in the case of Ag/Graphene/eGaIn[29] and 20 Ω for AgNP/SWCNT/eGaIn interfaces.[21] The sheet resistance of the AgNW/CNT layer was approximately 20 Ω sq^{-1} before eGaIn was applied, and it dropped to approximately 9 mΩ sq^{-1} in the case of our ACLM electrodes after the application of eGaIn (Figure S2). This result shows that our ACLM structure has good electrical contact between the constituting materials and the ACLM serves as a good conductor as a whole. One important property of our ACLM electrode is that the AgNWs in the ACLM electrode are very stable over time in contrast to the previous report.[10] Figure 2a shows the scanning electron microscope (SEM) image of the cross section of an ACLM electrode 7 days after the application of eGaIn. It shows that the AgNWs in the ACLM electrode remained intact and maintained their initial form under the contact of eGaIn. In the SEM image, SWCNTs were observed around the AgNWs in a network arrangement (Figure S3). We propose that these SWCNTs encapsulating AgNWs serve as a thin protection layer against eGaIn. Based on the energy-dispersive X-ray (EDX) image in Figure 2b, we can clearly confirm this effect. For EDX mapping, we dropped eGaIn on the filtered AgNW/SWCNT electrode. After 1 month, eGaIn was blown aside using N_2 gas to expose the AgNW/SWCNT surface (Base sample). In Figure 2b, the Ga layer and the In layer can be seen in the part where eGaIn is located in the Base sample. In the Ag layer, since AgNW is evenly distributed on the sample surface, the Ag L signal can be observed over the area. EDX mapping graph shows that Ga and In are unequally distributed in Ga L and In L, while Ag is uniformly distributed in Ag L. First, if AgNW is dissolved in Ga, the distribution of AgNW mapping and the distribution of Ga should be the same. In other words, when blowing with N_2, eGaIn and AgNW must be removed together. However, the two distributions were different, indicating that AgNWs were not dissolved by eGaIn. The localized Ag L signals appearing

https://doi.org/10.1021/acsomega.3c08246
ACS Omega 2024, 9, 3916−3922

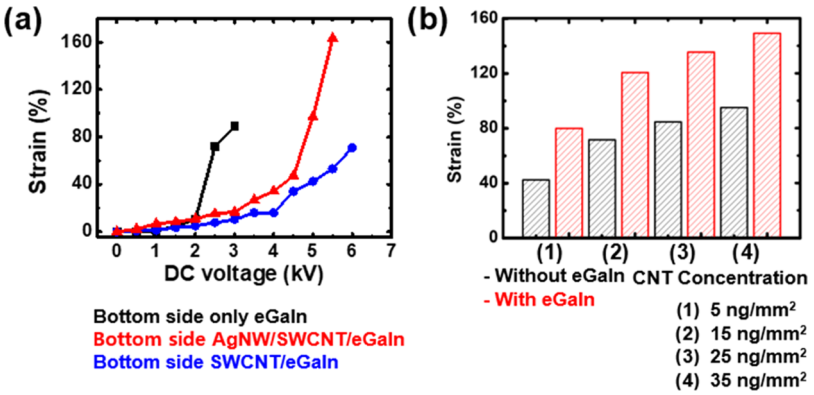

Figure 3. Characteristics of ACLM hybrid electrodes. (a) Stretchability performance in accordance with external DC voltage graph for three types of bottom electrodes: (black) eGaIn only, (red) AgNW/SWCNT/eGaIn, (blue) SWCNT/eGaIn. (b) Maximum strain versus external DC voltage for ACLM electrodes with different CNT concentrations. The black bars denote the maximum strains of AgNW/SWCNT electrodes without eGaIn. The red bars denote the maximum strains of the ACLM electrodes with eGaIn.

only on the exposed AgNW region are further supported by the localized EDX signals on the AgNW region (Figure S4).

The use of the ACML electrode further improved the stretchability and luminance performance of ELDEAs. Figure 3a shows the improvement in the stretchability performance as a function of the DC voltage. First, we transferred the optically transparent AgNW/SWCNT electrode to the top side of the DEA samples. We then transferred various types of electrodes to the bottom side. Three different types of bottom electrodes were prepared: eGaIn only, SWCNT/eGaIn hybrid structure, and ACLM electrode. AgNW/eGaIn electrodes were not considered because AgNWs were dissolved in eGaIn without the SWCNT protection layer.[30] In the case of the eGaIn-only bottom electrode, the DEA samples failed easily at a relatively lower DC voltage of 3 kV (Figure 3a, black). This is presumably due to the small thickness (50 μm) of the prestrained VHB tape and the increased probability of eGaIn penetration into the polymer film. Owing to the liquid property of eGaIn, it can penetrate the polymer matrix resulting in high electric fields, ultimately leading to failure.

In the case of the SWCNT/eGaIn electrode, we transferred the SWCNT film to the DEA, and then, we deposited eGaIn on the SWCNT layer. The existence of the SWCNT on the polymer increased the maximum applicable DC voltage level. The SWCNT/eGaIn electrode yielded the lowest stretchability performance of 71% out of the three cases (Figure 3a, blue). A larger breakdown voltage of ∼6 kV shows that the SWCNTs prevent the penetration of the eGaIn into the polymer matrix, resulting in the increased maximum strain. However, the SWCNTs constrained the mechanical stretching deformation of the underlying polymer, resulting in smaller strain values compared with ACLM electrodes. The ACLM electrode showed maximum strain of 163% (Figure 3a, red), which is larger than that of the other two cases. This is because the CNTs in the ACLM structure prevent the chemical reaction of AgNWs with eGaIn, while enabling the high mechanical stretchability of the electrode. This indicates that the concentration of SWCNT as well as eGaIn plays an important role in terms of mechanical performance. However, in the case of SWCNT concentration, it has the opposite effect on the mechanical and optical performance. This is because the incorporation of CNTs distributed the electrical stresses within the elastomer and increased the effective electric field density applied to the elastomer, resulting in an improved maximum breakdown field and strain.

The light-emitting performance of the ELDEA was largely affected by the transmittance of the AgNW/SWCNT and the reflectance from eGaIn at the ACLM electrode. Since the transmittance of the AgNW/SWCNT electrode decreases with the thickness of SWCNT we incorporate, we needed to optimize the SWCNT concentration for optimum optical and mechanical performance.[17] In the case of the ACLM electrodes, eGaIn showed good mechanical and electrical contact between the AgNW/SWCNT layer and eGaIn. The increase in the SWCNT concentration distributes the thermal and electrical stresses of the AgNW/SWCNT layer.[31] In addition, the increase in the SWCNT concentration can help to maintain the mechanical coupling between the AgNWs.[32] As can be observed by the black bars in Figure 3b, the higher the concentration of SWCNTs on the ACLM electrodes, the greater the maximum stretchability performance. However, an increase in the SWCNT concentration causes a decrease in transparency in the AgNW/SWCNT and eGaIn, which can also reduce the reflection efficiency. This is because electrodes exist on the top side and bottom side, but eGaIn is applied only on the bottom side, and therefore light emission occurs only on the top side. Here, we observed the optical transmittance of the stretchable electrodes. The transmittance of AgNW/SWCNT electrodes with different concentrations of SWCNTs was measured using a UV−vis spectrophotometer (Cary 8454, Agilent Technologies). The transmittance decreased from 100 to 88, 84, and 59% at CNT concentrations of 5, 15, and 35 ng mm^{-2}, respectively, at a 532 nm wavelength. In our devices, 5 ng mm^{-2} SWCNT concentration was used for the electrode to have both high transparency and stretchability (Figure S5). We can observe that the ACLM electrode with a low SWCNT concentration (5 ng mm^{-2}) attains approximately half of the strain compared to the ACLM electrode with an increased SWCNT amount (35 ng mm^{-2}). In ELDEA, when the SWCNT concentration increases, the transmittance of the electrodes decreases. Therefore, we chose the minimum SWCNT concentration (5 ng mm^{-2}) to maximize optical transparency and still obtain high strain values, as indicated in our previous publication.[17] The SWCNT concentration for the hybrid reflective ACLM electrode mentioned above led to enhancements in both the luminance and stretchability performances. We observed the

https://doi.org/10.1021/acsomega.3c08246
ACS Omega 2024, 9, 3916−3922

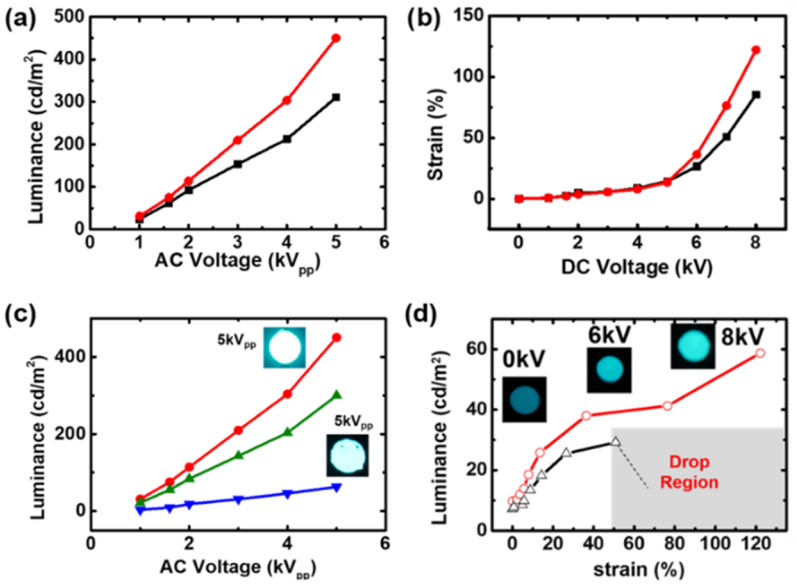

Figure 4. Luminance and stretchability performance of ACLM-ELDEA devices. (a) Luminance versus AC voltage signal graph. The red curve is ACML-ELDEA device luminance graph. The black curve is AgNW/SWCNT ELDEA device luminance graph. (b) Strain versus DC voltage signal graph. The black line depicts the use of the AgNW/SWCNT hybrid electrodes without eGaIn. The red line depicts the use of the ACLM hybrid electrodes with eGaIn. (c) Luminance as a function of AC voltage of samples with different SWCNT concentrations. The blue, green, and red data correspond to SWCNT concentrations of 35, 15, and 5 ng mm^{-2}, respectively. (d) Luminance versus Strain graph at 1 kV_{pp} AC and 1 kHz. The DC voltage was increased from 0 up to 8 kV. No luminance drop was observed for samples using ACLM electrodes.

electroluminescence with the use of our ACLM-ELDEA. We compared two samples with different bottom electrodes: one with the AgNW/SWCNT bottom electrode and the other with the ACLM bottom electrode. As shown in Figure 4a, by utilizing the ACLM bottom electrode, we were able to increase the maximum luminance of the ELDEA by 50%. The 50% loss can be attributed to the isotropic light emission from the electroluminescent ZnS:Cu particles, internal and interfacial reflection/absorption, and light scattering on the ACLM surface.[33] It should be noted that the use of ACLM electrodes lowered the required voltage levels to attain a given electroluminescence intensity compared with the case of AgNW/SWCNT electrodes. The maximum luminance of ELDEA with the AgNW/SWCNT electrode was 300 cd m^{-2} at 5 kV_{pp} (AC) and 4 kV (DC) (Figure 4a, black). The same luminance value of 300 cd m^{-2} can be achieved at voltages of 4 kV_{pp} (AC) and 4 kV (DC) using ACLM electrodes (Figure 4a, red). This shows that the eGaIn surface can serve as a stretchable reflector that increases the electroluminescence intensity toward the frontal direction. Furthermore, as shown in Figure 4b, the maximum attainable strain also increased by 44%, as expected from the results in Figure 2. The eGaIn is a liquid metal that allows the distribution of thermal and electrical stresses over conventional composite electrodes. Therefore, the ACLM-ELDEA had 122% maximum strain (red line), compared to the 85% composite strain at the previous ELDEA (black line).[10] Also, the use of the ACLM electrodes lowered the applied voltage level to attain the same level of strain compared with those devices that used the AgNW/SWCNT electrodes only. The maximum strain of using an AgNW/SWCNT electrode (Figure 4b, black) was 85%, achieved at a DC voltage of 8 kV. That maximum strain value of 85% can be obtained at 7.2 kV as indicated by the red line (reflective hybrid electrode). Electroluminance as a function of the AC voltage of ACLM-ELDEA samples with different bottom-side SWCNT concentrations was studied. We tested three SWCNT concentrations (5, 15, and 35 ng mm^{-2}), and the results are shown in Figure 4c. The maximum luminance was 63 cd m^{-2} for 35 ng mm^{-2} SWCNT concentration (Figure 4c, blue), compared to 450 cd m^{-2} for 5 ng mm^{-2} SWCNT concentration (Figure 4c, red). This confirms that luminance is reduced by an increased SWCNT concentration. Interestingly, the use of the ACLM reflective electrodes increased the luminance stability at high strains (Figure 4d). When we increase the DC signal voltage applied to the ELDEA device, we expected thickness reduction of the electroluminescent layer (electric field increase) together with a decrease in the areal concentration of electroluminescent particles (reduction of EL luminance). According to our previous work on ELDEAs with the use of AgNW/SWCNT electrodes on both sides, the luminance dropped steeply at strain values larger than 49.1% (gray area in Figure 4d).[10] This steep drop in luminance using AgNW/SWCNT electrodes can be attributed to (a) a decrease in the areal density of the electroluminescent particles and (b) the decreased ability to apply a uniform electric field inside the film. In this case, upon stretching, the distances among the AgNWs increased, and the area density of the AgNWs decreased accordingly. This resulted in a weaker average electric field in the film. However, for ACLM-ELDEAs, the devices show increased luminance stability, even at high DC voltage levels. This can be attributed to several factors. First, the luminance drop at high DC voltage levels was compensated by the increase of the luminance using an eGaIn reflection. Indeed, Figure 4d shows that the slope for strains in the range from 0 to 49.1% is larger than the slope for strain values larger than 49.1%. This means that when the DC voltage increases, the volume that the EL particles occupy decreases and a drop in luminance is induced. In our case, this drop was compensated for by using an ACLM electrode. Second, eGaIn helped in maintaining the high conductivity of ALCM electrodes even at high DC values. The lack of the

https://doi.org/10.1021/acsomega.3c08246
ACS Omega 2024, 9, 3916−3922

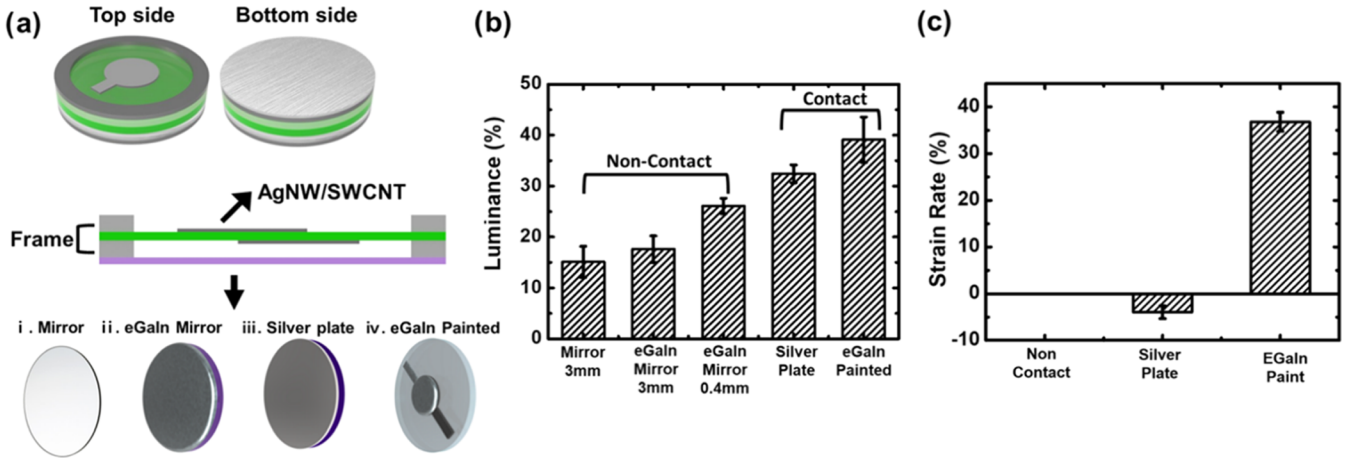

Figure 5. Various forms of reflectors attached on ELDEA. (a) Schematic of ELDEA and reflector assembly. Reflector mirror, eGaIn mirror, silver plate, and eGaIn painted. (b) Variation of reflector luminance for different noncontact and contact settings. In the noncontact section, the reflection area is separated from the AgNW/SWCNT electrode by 0.4 and 3 mm. On the other hand, in the contact section, the reflection area is attached to the AgNW/SWCNT electrode. (c) Strain variation for various contact reflectors. The control sample (noncontact) uses AgNW/SWCNT bottom electrode.

drop-region phenomenon is important for the proper operation of flexible devices.

We compared the reflective performance of the ACLM reflector with respect to other reflective surfaces, such as a commercial mirror, Ag-coated silicon wafer, and eGaIn-coated wafer (Figure 5a). The experiment was performed in noncontact mode using samples with AgNW/SWCNT electrodes on both sides by placing the reflective planes below the bottom electrode. The luminance increase was minimal for the commercial mirror at a 3 mm separation from the bottom electrode. Next was the eGaIn-coated Si wafer as the reflector. The percentile luminance increase was 18 and 26%, respectively, for distances of 3 and 0.4 mm between the bottom electrode and reflector surface (Figure 5b, noncontact). Next, contact-mode experiments were performed for two cases (Figure 5b, contact). For the first case, a silver plate was made in direct contact with the bottom electrode. This resulted in a 33% increase in luminance. However, when the ACLM bottom electrode was used, the luminance increase showed a maximum value of 40%. (Figure 5b).

A silver plate is a good reflector, but it has negligible stretchability. Indeed, the contact of a silver plate with the bottom electrode resulted in an actual decrease in strain by 4% (Figure 5c, center). In contrast, the application of eGaIn to the AgNW/SWCNT bottom electrode (ACLM electrode) resulted in a maximum strain increase of 39.1% (Figure 5c, right). This is due to the low viscosity (about 2 times that of water) of eGaIn,[34] which results in a negligible effect on the stretchability of the device. This shows that eGaIn with its low viscosity does not decrease the stretchability performance of ELDEA. In fact, it improves the electrode performance and increases the ELDEA strain.

4. CONCLUSIONS

In conclusion, we reported on the strategy of enhancing electroluminescence and actuating abilities by combining liquid eutectic gallium indium metal with a stretchable and transparent hybrid electrode composed of AgNWs and SWCNTs. We demonstrated that the maximum luminance and maximum strain of the electroluminescent dielectric elastomer actuator increased by 50% (from 300 to 450 cd m^{-2}) and by 44% (from 85 to 122%), respectively. The device showed improved optical properties, electrical conductivity, and stability for electroluminescent dielectric elastomer actuators compared with previous works. Our strategy can be easily applied to frameless DEAs in the future. We expect that this strategy will impact soft skin and muscle development for use in soft robotics. Actuators that can take colors or emit light can also be used in diverse fields such as home appliances that can change color according to consumer needs. Another field would be rescue or deep sea missions where actuators can also provide light to the ambient.

■ ASSOCIATED CONTENT

Supporting Information

The Supporting Information is available free of charge at https://pubs.acs.org/doi/10.1021/acsomega.3c08246.

Four-point probe measurement configuration, sheet resistance measurement, SEM and EDX image of electrode, and transmittance characteristics of AgNW/SWCNT electrode (PDF)

■ AUTHOR INFORMATION

Corresponding Author

Byung Yang Lee − *Department of Mechanical Engineering, Korea University, Seoul 02841, Republic of Korea;* orcid.org/0000-0003-0125-2501; Email: blee@korea.ac.kr

Authors

Jongyeop An − *Department of Mechanical Engineering, Korea University, Seoul 02841, Republic of Korea*

Beomgil Ha − *Department of Mechanical Engineering, Korea University, Seoul 02841, Republic of Korea*

Seon Namgung − *Department of Physics, Ulsan National Institute of Science and Technology, Ulsan 44919, Republic of Korea*

Complete contact information is available at: https://pubs.acs.org/10.1021/acsomega.3c08246

https://doi.org/10.1021/acsomega.3c08246
ACS Omega 2024, 9, 3916−3922

Author Contributions

[§]J.A. and B.H. contributed equally to this paper.

Notes

The authors declare no competing financial interest.

■ ACKNOWLEDGMENTS

This project was supported by the National Research Foundation (NRF) funded by the Korea Ministry of Science and ICT (2021R1A2C2014088). This project was also supported by Korea Environment Industry & Technology Institute (KEITI) through Technology Development Project for Biological Hazards Management in Indoor Air Program (or Project) funded by Korea Ministry of Environment (RE202101004).

■ REFERENCES

(1) Cai, L.; Zhang, S.; Miao, J.; Yu, Z.; Wang, C. Fully printed stretchable thin-film transistors and integrated logic circuits. *ACS Nano* **2016**, *10* (12), 11459−11468.
(2) Duduta, M.; Wood, R. J.; Clarke, D. R. Multilayer dielectric elastomers for fast, programmable actuation without prestretch. *Adv. Mater.* **2016**, *28* (36), 8058−8063.
(3) Kim, C.-C.; Lee, H.-H.; Oh, K. H.; Sun, J.-Y. Highly stretchable, transparent ionic touch panel. *Science* **2016**, *353* (6300), 682−687.
(4) Liang, J.; Li, L.; Chen, D.; Hajagos, T.; Ren, Z.; Chou, S.-Y.; Hu, W.; Pei, Q. Intrinsically stretchable and transparent thin-film transistors based on printable silver nanowires, carbon nanotubes and an elastomeric dielectric. *Nat. Commun.* **2015**, *6* (1), No. 7647.
(5) Wang, J.; Yan, C.; Cai, G.; Cui, M.; Lee-Sie Eh, A.; See Lee, P. Extremely stretchable electroluminescent devices with ionic conductors. *Adv. Mater.* **2016**, *28* (22), 4490−4496.
(6) Lee, H.; Kim, M.; Kim, I.; Lee, H. Flexible and stretchable optoelectronic devices using silver nanowires and graphene. *Adv. Mater.* **2016**, *28* (22), 4541−4548.
(7) Keplinger, C.; Sun, J.-Y.; Foo, C. C.; Rothemund, P.; Whitesides, G. M.; Suo, Z. Stretchable, transparent, ionic conductors. *Science* **2013**, *341* (6149), 984−987.
(8) Bu, T.; Xiao, T.; Yang, Z.; Liu, G.; Fu, X.; Nie, J.; Guo, T.; Pang, Y.; Zhao, J.; Xi, F.; et al. Stretchable triboelectric−photonic smart skin for tactile and gesture sensing. *Adv. Mater.* **2018**, *30* (16), No. 1800066.
(9) Wang, J.; Yan, C.; Chee, K. J.; Lee, P. S. Highly stretchable and self-deformable alternating current electroluminescent devices. *Adv. Mater.* **2015**, *27* (18), 2876−2882.
(10) Lee, Y. R.; An, J.; Kim, H. S.; Park, I. W.; Heo, K.; Lee, H.; Lee, B. Y. Electroluminescent soft elastomer actuators with adjustable luminance and strain. *Soft Matter* **2019**, *15* (40), 7996−8000.
(11) Wang, Y.; Zhang, L.; Wang, D. Ultrastretchable hybrid electrodes of silver nanowires and multiwalled carbon nanotubes realized by capillary-force-induced welding. *Adv. Mater. Technol.* **2019**, *4* (11), No. 1900721.
(12) Wang, Y.; Kong, X.; Gao, J.; Gong, M.; Lin, X.; Zhang, L.; Guo, M.; Wang, D. Customizable stretchable transparent electrodes based on AgNW/CNT hybrids via tailoring sizes of building blocks. *ACS Appl. Electron. Mater.* **2022**, *4* (3), 1186−1195.
(13) Cochran, C. N.; Foster, L. Vapor pressure of gallium, stability of gallium suboxide vapor, and equilibria of some reactions producing gallium suboxide vapor. *J. Electrochem. Soc.* **1962**, *109* (2), 144.
(14) Dickey, M. D. Stretchable and soft electronics using liquid metals. *Adv. Mater.* **2017**, *29* (27), No. 1606425.
(15) Zrnic, D.; Swatik, D. On the resistivity and surface tension of the eutectic alloy of gallium and indium. *J. Less Common Met.* **1969**, *18* (1), 67−68.
(16) Palleau, E.; Reece, S.; Desai, S. C.; Smith, M. E.; Dickey, M. D. Self-healing stretchable wires for reconfigurable circuit wiring and 3D microfluidics. *Adv. Mater.* **2013**, *25* (11), 1589−1592.
(17) Lee, Y. R.; Kwon, H.; Lee, D. H.; Lee, B. Y. Highly flexible and transparent dielectric elastomer actuators using silver nanowire and carbon nanotube hybrid electrodes. *Soft Matter* **2017**, *13* (37), 6390−6395.
(18) Mohammed, M.; Sundaresan, R.; Dickey, M. D. Self-running liquid metal drops that delaminate metal films at record velocities. *ACS Appl. Mater. Interfaces* **2015**, *7* (41), 23163−23171.
(19) Wu, Q.; Zou, S.; Gosselin, F. P.; Therriault, D.; Heuzey, M.-C. 3D printing of a self-healing nanocomposite for stretchable sensors. *J. Mater. Chem. C* **2018**, *6* (45), 12180−12186.
(20) Glickman, E.; Levenshtein, M.; Budic, L.; Eliaz, N. Interaction of liquid and solid gallium with thin silver films: Synchronized spreading and penetration. *Acta Mater.* **2011**, *59* (3), 914−926.
(21) Oh, E.; Kim, T.; Yoon, J.; Lee, S.; Kim, D.; Lee, B.; Byun, J.; Cho, H.; Ha, J.; Hong, Y. Highly Reliable Liquid Metal−Solid Metal Contacts with a Corrugated Single-Walled Carbon Nanotube Diffusion Barrier for Stretchable Electronics. *Adv. Funct. Mater.* **2018**, *28* (51), No. 1806014, DOI: 10.1002/adfm.201870361.
(22) Hu, L.; Wang, L.; Ding, Y.; Zhan, S.; Liu, J. Manipulation of liquid metals on a graphite surface. *Adv. Mater.* **2016**, *28* (41), 9210−9217.
(23) Bury, E.; Chun, S.; Koh, A. S. Recent advances in deformable circuit components with liquid metal. *Adv. Electron. Mater.* **2021**, *7* (4), No. 2001006.
(24) Zrudsky, D. R.; Bush, H. D.; Fassett, J. R. Four point sheet resistivity techniques. *Rev. Sci. Instrum.* **1966**, *37* (7), 885−890.
(25) Kim, J. S.; Cho, S. H.; Kim, K. L.; Kim, G.; Lee, S. W.; Kim, E. H.; Jeong, B.; Hwang, I.; Han, H.; Shim, W.; et al. Flexible artificial synesthesia electronics with sound-synchronized electroluminescence. *Nano Energy* **2019**, *59*, 773−783.
(26) Xuan, H. D.; Timothy, B.; Park, H. Y.; Lam, T. N.; Kim, D.; Go, Y.; Kim, J.; Lee, Y.; Ahn, S. I.; Jin, S. H.; Yoon, J. Super Stretchable and Durable Electroluminescent Devices Based on Double-Network Ionogels. *Adv. Mater.* **2021**, *33* (25), No. 2008849.
(27) Gu, M.; Chen, Y.; Gu, S.; Wang, C.; Chen, L.; Shen, H.; Chen, G.; Sun, X.; Huang, H.; Zhou, Y.; Wen, Z. Brightness-enhanced electroluminescence driven by triboelectric nanogenerators through permittivity manipulation and impedance matching. *Nano Energy* **2022**, *98*, No. 107308.
(28) Webster, J. G.; Pallas-Areny, R. *Design for Biomedical Engineers*; Wiley, 2003.
(29) Secor, E. B.; Cook, A. B.; Tabor, C. E.; Hersam, M. C. Wiring up liquid metal: Stable and robust electrical contacts enabled by printable graphene inks. *Adv. Electron. Mater.* **2018**, *4* (1), No. 1700483.
(30) Campbell, A. N.; Reynolds, W. The system silver−indium−gallium. *Can. J. Chem.* **1962**, *40* (1), 37−45.
(31) Lee, M.-S.; Lee, K.; Kim, S.-Y.; Lee, H.; Park, J.; Choi, K.-H.; Kim, H.-K.; Kim, D.-G.; Lee, D.-Y.; Nam, S.; Park, J. U. High-performance, transparent, and stretchable electrodes using graphene−metal nanowire hybrid structures. *Nano Lett.* **2013**, *13* (6), 2814−2821.
(32) Pyo, J. B.; Kim, B. S.; Park, H.; Kim, T. A.; Koo, C. M.; Lee, J.; Son, J. G.; Lee, S.-S.; Park, J. H. Floating compression of Ag nanowire networks for effective strain release of stretchable transparent electrodes. *Nanoscale* **2015**, *7* (39), 16434−16441.
(33) Bredol, M.; Schulze Dieckhoff, H. Materials for powder-based AC-electroluminescence. *Materials* **2010**, *3* (2), 1353−1374.
(34) Spells, K. E. The determination of the viscosity of liquid gallium over an extended nrange of temperature. *Proc. Phys. Soc.* **1936**, *48* (2), 299.

https://doi.org/10.1021/acsomega.3c08246
ACS Omega 2024, 9, 3916−3922